Harmful Algae 130 (2023) 102544

Contents lists available at ScienceDirect

Harmful Algae

journal homepage: www.elsevier.com/locate/hal

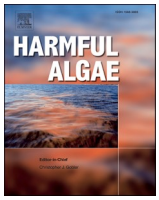

Does prey availability influence the detection of *Dinophysis* spp. by the imaging FlowCytobot?

Emilie Houliez [a,*], Alexis D. Fischer [b], Brian D. Bill [c], Stephanie K. Moore [d]

[a] *Fulbright Scholar sponsored by the Franco-American Fulbright Commission and Guest Researcher at the Northwest Fisheries Science Center, National Marine Fisheries Service, National Oceanic and Atmospheric Administration, Seattle, WA, 98112, United States of America*
[b] *University Corporation for Atmospheric Research, under contract to Northwest Fisheries Science Center, National Marine Fisheries Service, National Oceanic and Atmospheric Administration, Seattle, WA, 98112, United States of America*
[c] *Environmental and Fisheries Science Division, Northwest Fisheries Science Center, National Marine Fisheries Service, National Oceanic and Atmospheric Administration, Seattle, WA, 98112, United States of America*
[d] *Conservation Biology Division, Northwest Fisheries Science Center, National Marine Fisheries Service, National Oceanic and Atmospheric Administration, Seattle, WA, 98112, United States of America*

ARTICLE INFO

Edited by Dr. C. Gobler

Keywords:
Imaging FlowCytobot
Harmful algal bloom
Dinophysis
Mesodinium
Mixotroph

ABSTRACT

The Imaging FlowCytobot (IFCB) is a field-deployable imaging-in-flow cytometer that is increasingly being used to monitor harmful algae. The IFCB acquires images of suspended particles based on their chlorophyll-*a* fluorescence and/or the amount of light they scatter (side scattering). The present study hypothesized that fluorescence-based image acquisition would undercount *Dinophysis* spp., a genus of non-constitutive mixotrophs, when prey is limited. This is because *Dinophysis* spp. acquire plastids via ingestion of their ciliate prey *Mesodinium* spp., and lose photosynthetic capacity and autofluorescence in the absence of prey. Even small blooms of *Dinophysis* spp. can be highly toxic and result in diarrhetic shellfish poisoning (DSP), highlighting the importance of accurately detecting low abundances. To explore this, laboratory experiments were conducted to determine optimal IFCB settings for a fed culture of *Dinophysis acuminata*, and an existing time series of IFCB observations collected in Puget Sound (Washington, U.S.A) was used to compare *Dinophysis* spp. abundance estimates from samples triggered via side scattering versus fluorescence in relation to *Mesodinium* spp. abundance. This study introduces a quantitative approach for optimizing the detection of target harmful algae which can be repeated across multiple IFCBs and demonstrates the effects of IFCB calibration on *Dinophysis* spp. detection. The laboratory experiments showed that IFCB settings for fluorescence-based image acquisition need to be fairly sensitive to accurately detect *D. acuminata* cells. A poorly calibrated IFCB can miss a significant proportion of *D. acuminata* abundance whatever the method used to trigger the image acquisition. Field results demonstrated that the physiological status of *Dinophysis* spp. can influence their detection by the IFCB when triggering on fluorescence. This was observed during a 7-day period when the IFCB failed to detect *Dinophysis* spp. cells when triggering on fluorescence while cells were still detected using the side scattering triggering method as well as observed by microscopy. During this period, *Mesodinium* spp. was not detected, IFCB-derived autofluorescence level of individual cells of *Dinophysis* spp. was low, and less than 50 % of *Dinophysis* spp. cells exhibited autofluorescence under the microscope. Together, this indicates that the unique feeding ecology of *Dinophysis* spp. may affect their detection by the IFCB when cells are starved.

1. Introduction

Harmful algal blooms (HABs) threaten human health and coastal economies through the production of toxins and other bioactive compounds. In marine systems, one of the most effective ways to reduce or eliminate the societal impacts of HABs is to provide early warning (Brown et al., 2012). Adequate early warning enables mitigation strategies to be put into place to prevent human exposures to HAB toxins and minimize economic losses that may be associated with management strategies designed to protect human health (Anderson et al., 2001; Jin and Hoagland 2008). HAB early warning is most often provided through microscopy-based monitoring of the causative organisms that triggers

* Corresponding author.
E-mail address: emilie.houliez@fulbrightmail.org (E. Houliez).

https://doi.org/10.1016/j.hal.2023.102544
Received 9 August 2023; Received in revised form 5 November 2023; Accepted 13 November 2023
Available online 15 November 2023
1568-9883/Published by Elsevier B.V.

some management response (e.g., toxin testing in shellfish tissues or proactive shellfish harvest closures) when abundance thresholds are exceeded (Belin et al., 2021; Trainer and King 2023; Trainer and Suddleson 2005). However, because traditional microscopy-based monitoring methods are labor intensive, sample collection is often conducted on weekly or biweekly timescales that are not always adequate for detecting rapidly developing HABs. This can shorten the opportunity to provide early warning which increases risk to the public for toxin exposure and/or the likelihood of costly recalls of contaminated shellfish, especially for HABs that cause toxicity at low abundances. Dinoflagellates in the genus *Dinophysis* can produce toxins (collectively called diarrhetic shellfish toxins [DSTs]) that cause the syndrome diarrhetic shellfish poisoning (DSP) in humans (Reguera et al., 2014; Reguera et al., 2012) at low abundances less than ~200 cells L^{-1} (Yasumoto et al., 1985). To address this problem, new technologies are increasingly being used to rapidly and autonomously detect developing HABs *in situ* (Anderson et al., 2012; Glibert et al., 2018).

One such technology is the Imaging FlowCytobot (IFCB). The IFCB is a field-deployable, imaging-in-flow cytometer that continuously captures high-resolution images of particles taken from aquatic environments. It samples and analyzes nominal 5 mL water samples approximately every 20 min, providing valuable data on the size, shape and autofluorescence characteristics of the imaged particles, over deployments that can last up to several months (Olson and Sosik 2007). When the IFCB is paired with a machine learning image classifier, this system can count and identify multiple HAB species and other phytoplankton (between ~10–150 micrometers in size) to the genus-level and sometimes species-level with demonstrated accuracy comparable to that of human experts (Sosik and Olson 2007). The IFCB is a powerful tool for advancing early warning of HABs that is rapidly gaining popularity. At the time of this writing, a total of 103 IFCBs are in use worldwide and 53 % of them were acquired during the four last years. In California coastal waters, a statewide network of 12 IFCBs is currently being used to implement an automated early warning system for the detection of HABs at 9 critical land-based locations in addition to four research cruises (Kudela et al., 2021; https://sccoos.org/ifcb/).

A notable example of an IFCB providing HAB early warning is when an IFCB deployed in Port Aransas, Texas detected a *Dinophysis* spp. bloom ahead of the 2008 Rockport Oysterfest – which attracted up to 30,000 people – and prompted alerts to shellfish managers that likely averted an outbreak of DSP (Campbell et al., 2010). While HABs of *Dinophysis* spp. have been documented in Western Europe, Chile, Perú, and Japan since the 1970s (Reguera et al., 2014), they were not known to cause harm in the U.S. until the 2008 event (Anderson et al., 2021). The first conclusive cases of DSP in the U.S. occurred in 2011 when a family was sickened after consuming recreationally harvested mussels from Puget Sound, Washington (Lloyd et al., 2013; Trainer et al., 2013). Today, shellfish harvesting closures due to unsafe levels of DSTs are enforced annually at multiple sites throughout the U.S. and *Dinophysis* spp. are considered an emerging threat (Anderson et al., 2021; Ayache et al., 2023; Hattenrath-Lehmann et al., 2013). In recognition of this, investments have been made to establish a national network of IFCBs to better understand *Dinophysis* spp. HABs and their drivers (NCCOS and US IOOS 2020). With the expanded use of IFCBs to provide early warning of HABs of *Dinophysis* spp., it is becoming increasingly important to identify factors that might affect their performance.

The IFCB can be configured to detect particles using side scattering (which depends on the size of the particle) and/or laser-induced chlorophyll-*a* fluorescence. Particle detection using side scattering detects all particles that scatter light, including detritus, the abundance of which generally greatly exceeds that of phytoplankton in coastal systems (Olson and Sosik 2007). Fluorescence-based particle detection only images particles with chlorophyll-*a* and is more often used for HAB (and phytoplankton) monitoring and detection. Different approaches for tuning the IFCB include adjusting settings to image as wide a size range of phytoplankton as possible (e.g., Neeley et al., 2021), or to maximize detection of target (HAB) species - however, the latter is rarely done in a quantitative way. Non-optimal IFCB settings are likely to undercount target HAB species, thereby compromising the ability of the IFCB to provide early warning of HABs, particularly if mitigation actions depend on species abundances exceeding specified management thresholds.

Even with a well-tuned IFCB, fluorescence-based detection of *Dinophysis* spp. may be complicated by its unique feeding ecology. *Dinophysis* spp. are non-constitutive mixotrophs and combine phototrophy and heterotrophy. They lack permanent plastids (chloroplasts) and must acquire them via ingestion of the ciliate *Mesodinium* spp. that itself steals them by feeding on cryptophytes belonging to the *Teleaulax-Plagioselmis-Germinigera* (TPG) clade (Hansen et al., 2013; Park et al., 2006; Park et al., 2008). The size of *Mesodinium* spp. and time lag between *Mesodinium* spp. and *Dinophysis* spp. blooms both influence *Dinophysis* spp. physiological status and formation of intense blooms (Harred and Campbell 2014; Smith et al., 2018). Though *Dinophysis* spp. can survive extended periods without prey (up to three months), they must regularly feed to sequester new plastids to maintain optimal growth and their ability to photosynthesize (Kim et al., 2012; Park et al., 2008). In the absence of prey, the photosynthetic capacity and autofluorescence of *Dinophysis* spp. progressively decrease (Park et al., 2008), which could compromise the ability of the IFCB to accurately detect these cells. Despite declining growth rates and photosynthetic capacity, toxin production continues during starvation leading to increased cellular toxicity (García-Portela et al., 2018; Nielsen et al., 2012; Nielsen et al., 2013). Due to the acute health risk posed by starved *Dinophysis* spp cells, it is important to accurately detect cells with reduced autofluorescence.

The goal of this study was to determine if the ability of the IFCB to detect *Dinophysis* spp. varies due to different physiological characteristics of cells related to prey availability. It was hypothesized that the IFCB fluorescence-based image acquisition would undercount *Dinophysis* spp. cells exhibiting weak autofluorescence when prey is limited. To explore this, laboratory experiments were conducted to determine optimal settings of the IFCB for a culture of *Dinophysis acuminata*, and an existing time series of IFCB observations collected in Puget Sound was used to compare *Dinophysis* spp. abundance estimates from samples triggered via side scattering and fluorescence in relation to *Mesodinium* spp. abundance.

2. Materials and methods

2.1. Optimization of IFCB settings

Laboratory experiments were conducted to identify the optimal IFCB configuration settings for detecting *Dinophysis* spp. and to assess the adequacy of IFCB settings used to obtain the existing time series in Puget Sound. Both time series and laboratory measurements were collected with the same IFCB. *D. acuminata* was chosen for the experiment because it is commonly found in Puget Sound (Ayache et al., 2023; Trainer et al., 2013). However, because no established cultures of local strains of *D. acuminata* were available, the experiments were conducted using the DANY1 strain isolated from the Peconic Estuary, Long Island Sound, NY in May 2013. *D. acuminata* was maintained under favorable growth conditions following the methodology of Park et al. (2006) using the ciliate *Mesodinium rubrum* as prey. *D. acuminata* was grown in 0.22 μm filtered natural seawater (salinity 25, 18 °C) and fed twice a week with a Japanese strain of *M. rubrum* (JAMR). *M. rubrum* was grown in F/6-Si (salinity 25, 15 °C) and was fed once a week with a Japanese strain of the cryptophyte *Teleaulax amphioxeia* (JATA) that was grown in L1-Si (salinity 22, 18 °C). All cultures were grown under white light of ~100 μmol photons m^{-2} s^{-1} intensity and with a 12:12 light:dark cycle. Prior to the start of the experiment, cultured *D. acuminata* cells were observed to fluoresce under green light excitation (546 nm) using an inverted optical microscope (Axiovert 135, Zeiss, Germany) equipped with an epifluorescence module.

Optimal gain and threshold settings were identified for the two separate photomultiplier tubes (PMTs), one for side scattering and the other for fluorescence, that are used to trigger IFCB image acquisition. The gain (called PMT A for side scattering and PMT B for fluorescence) is used to adjust the sensitivity of the PMT while the threshold (called trig A for side scattering and trig B for fluorescence) determines the minimum value that the side scattering or fluorescence signal needs to reach in order to trigger imaging of the particle by the camera. Higher gains and lower thresholds will increase sensitivity for detecting and capturing images of smaller particles (when side scattering triggers image acquisition) or particles containing less chlorophyll (when fluorescence triggers image acquisition), but at the cost of higher noise. Higher gain settings can also reduce dynamic range as large particles may saturate the PMT signal. High detection sensitivity (i.e., higher gains and lower thresholds), combined with a high abundance of particles, can reduce the effective volume analyzed per sample due to high inhibit time. Inhibit time is the amount of time that the IFCB is unable to image new particles in the flow cell because it is busy imaging the previously detected particle (IFCB image acquisition is limited to ~14 images per second). Samples with high inhibit time can lead to very low total volumes analyzed per sample resulting in less accurate estimates of target species abundances. Adjusting the gain and threshold settings is therefore a balance of offering sufficient sensitivity to detect target species while limiting the detection of non-target/uninteresting particles and avoiding saturation of the PMT signal.

A series of IFCB measurements were made on the same *D. acuminata* (DANY1) culture. Due to the wide-range of possible PMT setting combinations on the IFCB, a preliminary study was performed on the *D. acuminata* culture to select the most appropriate range of PMT gain and threshold settings to quantitatively evaluate performance during the experiment. As a first pass, the threshold was set to a low value (0.125 V) and a broad range of PMT gains were iteratively tested by changing the PMT gain with a coarse resolution (0.1 V increasing steps), while the IFCB was analyzing the culture. It was observed that *D. acuminata* cells were poorly or not detected with gain values lower than 0.3 for PMT A and 0.6 for PMT B. These preliminary results were used to select the range over which the detection of *D. acuminata* was quantitatively evaluated. For each PMT channel (PMT A and PMT B), a total of 12 settings were quantitatively evaluated, each corresponding to a gain and threshold combination. Four PMT B gains (0.60, 0.70, 0.80, and 0.90 V) were combined with three threshold (trig B) settings (0.125, 0.140, and 0.160 V), and four PMT A gains (0.30, 0.40, 0.50, and 0.60 V) were combined with three threshold (trig A) settings (0.16, 0.20, and 0.25 V). To avoid any potential interaction of the two channels, PMT A and trig A were both set to zero volts when measurements were made using the PMT B channel and vice versa. For each combination of gain and threshold settings, the IFCB was set to analyze 1 mL. Before each sample, the sample tube was flushed and the intake line was primed with 1 mL of the sample to prevent carryover from the prior sample. For each combination of settings, the IFCB measurements were made in triplicate by measuring three separate 1 mL samples. All measurements were made within 2 days (one day for all measurements with side scattering and a second day for all measurements with fluorescence) to ensure that the *D. acuminata* culture remained consistent across samples. The cellular biovolume of *D. acuminata* is lower than other species of *Dinophysis* found in Puget Sound, and strains of *D. acuminata* isolated from the Northeast/Mid-Atlantic coast (including DANY1) have a lower biovolume compared to strains from the Pacific Northwest (Ayache et al., 2023). Therefore, the optimal IFCB settings identified during the experiments are conservative and likely more sensitive than what is required to detect the suite of *Dinophysis* species in Puget Sound. The abundance of *D. acuminata* DANY1 in the culture was also determined microscopically on each day of the IFCB measurements. A sample of the culture was fixed with 70 % ethanol and all of the *Dinophysis* spp. cells were counted in 1 mL sub-samples by observing the gridded Sedgwick Rafter chamber in its totality under an inverted optical microscope (Axiovert 135, Zeiss, Germany) at 100x magnification.

2.2. *In situ Dinophysis spp. observations*

2.2.1. *Study site*

This study leveraged an existing time series of IFCB observations in Puget Sound collected as part of a larger cross-regional comparison of *Dinophysis* spp. bloom dynamics in the U.S. The study site is located at the terminal end of Budd Inlet in southern Puget Sound, Washington State (Fig. 1). This area is both a hotspot for *Dinophysis* spp. blooms (Trainer and King 2023; Trainer et al., 2013) and a top shellfish producing region contributing up to 37 % of total production and almost 58 % of the $270 million total value in Washington State (Washington Sea Grant 2015). Washington's highest recorded value of DST (250 μg DST / 100 g of shellfish) was measured in blue mussels from Budd Inlet in 2016 (PSEMP Marine Waters Workgroup 2017) - a value well above the federal standard for human consumption of 16 μg/ 100 g of shellfish (FDA 2011).

Budd Inlet, located near the city of Olympia, is a narrow, elongated inlet that stretches approximately 2.5 km wide by 11 km long. The inlet is shallow with less than 11 m depth in the south and 27 m depth in the north. Tides are semidiurnal with an average range of 4.4 m. The southern part of Budd Inlet receives freshwater from the Deschutes River which flows through the Capitol Lake dam while the northern part receives seawater from South Puget Sound. The tide tends to create counter-clockwise flow patterns and sometimes a gyre forms in the center of Budd Inlet (Boatman et al., 2000).

2.2.2. *Puget Sound IFCB deployment*

The IFCB was deployed from a floating boathouse at the Olympia Yacht Club from March 31 to September 27, 2022. The IFCB intake was located at 1.7 m depth and was terminated with a 1-mm copper pre-filter followed by a 150 μm Nitex mesh to prevent biofouling and large particles from clogging the internal fluidics system. The IFCB was configured to continuously analyze 5 mL samples and to alternate between side scattering and fluorescence-based image acquisition. Fluorescence (PMT $B = 0.60$ V and trig $B = 0.125$ V) was primarily used to trigger image acquisition, with samples analyzed using side scattering (PMT $A = 0.50$ V and trig $A = 0.250$ V) to trigger image acquisition interspersed throughout the deployment approximately twice a day (every 30 samples). The IFCB observations were served on an IFCB dashboard hosted by the Harmful Algal Bloom Observing Network (https://habon-ifcb.whoi.edu/buddinlet).

A classifier that automates taxonomic classification of images was not used in this study. Instead, for each day of the deployment, one side scatter sample and the fluorescence sample immediately preceding or following it (206 samples total) were visually inspected and manually identified using publicly available MATLAB-based annotation tools (https://github.com/hsosik/ifcb-analysis). *Dinophysis* spp. cells were manually classified to the species level when possible or to genus level if their orientation did not provide a view of distinguishing criteria required for their identification (e.g., when they were pictured in apical or antapical views or when their left sulcal list was not clearly visible). This enabled the accurate counting and identification of the different *Dinophysis* species in the samples; something which can sometimes be difficult to reach with a classifier.

Measures of the level of autofluorescence of each phytoplankton cell that was sampled by the IFCB (IFCB-autofluorescence) were extracted from the adc files (PMT B column). Of note, these measures are available for each cell regardless of the method used to trigger image acquisition such that IFCB-autofluorescence measures were also obtained when the triggering method was side scattering (and vice versa).

Biovolume of each phytoplankton cell was extracted from the features files by following the blob and features extraction procedure (v2) available on github (https://github.com/hsosik/ifcb-analysis). This procedure implements the Moberg and Sosik (2012) algorithm that uses

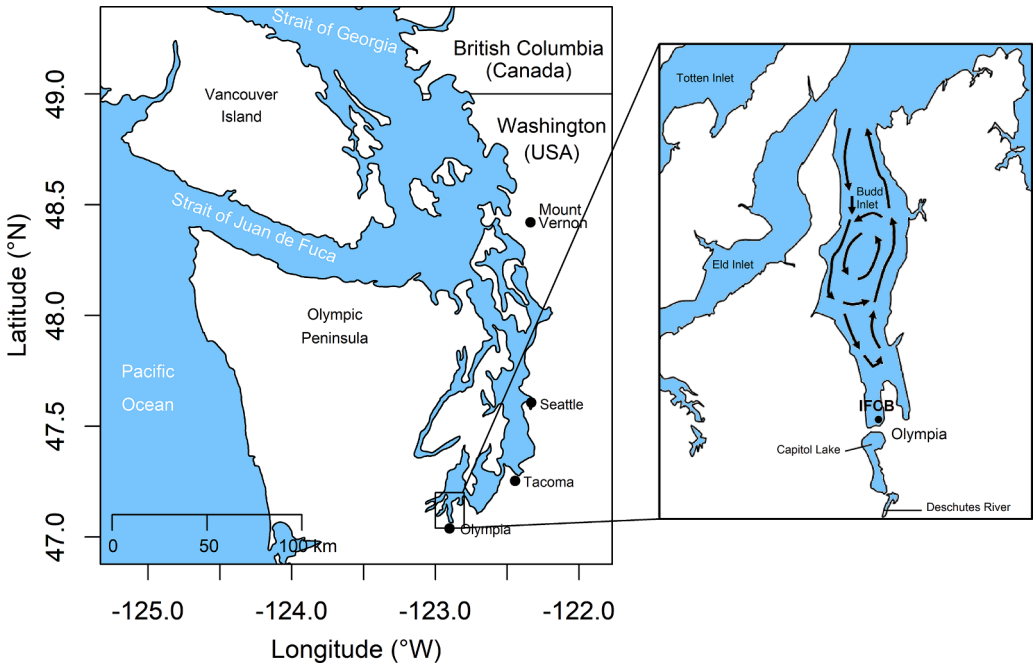

Fig. 1. Map of Puget Sound and inlet showing Budd Inlet with location of the imaging FlowCytobot (IFCB) deployment. Arrows represent water circulation.

distance maps to estimate cell volume from two-dimensional plankton images. Biovolume was converted from pixels to μm^3 using an estimated conversion factor of 3.81 pixels/micron determined from more than 1000 IFCB images of 5.7 μm fluorescent beads collected on different dates during the deployment.

To compare the IFCB measurements to conventional microscopy, discrete water samples were manually collected approximately weekly for observations of *Dinophysis* spp. cells, resulting in 18 samples total. A 2-L Niskin bottle was used to collect water samples at 1.5 m depth, which was slightly shallower than the placement of the IFCB intake. This sampling depth was chosen because it was where the highest chlorophyll concentrations were most often observed during preliminary sampling. Immediately upon returning to the laboratory, the discrete water sample was fixed with 70 % ethanol and *Dinophysis* spp. cells were enumerated at 100 x magnification using an inverted optical microscope (Axiovert 135, Zeiss, Germany) equipped with an epifluorescence module. To enable better comparison with the IFCB and match the 5 mL that the IFCB was configured to sample, all of the *Dinophysis* spp. cells were enumerated microscopically in a 5 mL sample without concentrating the sample and without replication. Five 1 mL sub-samples were transferred to a gridded Sedgwick Rafter chamber and each *Dinophysis* species was counted under the microscope and summed across sub-samples. The proportion of *Dinophysis* spp. cells exhibiting autofluorescence was also determine by microscopy under green light excitation with a fluorescence cube equipped with a green H 546 filter (excitation 546 nm).

2.3. Statistical analyses

2.3.1. Optimization of IFCB settings

Two-way ANOVAs followed by post-hoc pairwise multiple comparisons using the Holm–Šidák method (Holm 1979) were employed to assess the effects of the different gain and threshold settings, and their interactions, on the effective sample volume analyzed by the IFCB and IFCB estimates of *D. acuminata* abundances and total number of particles. Separate two-way ANOVAs were conducted for the side scattering (PMT A) and fluorescence-based (PMT B) triggering methods. Separate one-way ANOVAs (for PMT A and PMT B) followed by post-hoc multiple comparisons versus a control group with the Holm–Šidák method (Holm 1979) were used to test for differences between *D. acuminata* cell abundances determined by microscopy and the IFCB measurements made using the 12 PMT gain and threshold setting combinations. Before ANOVA analyses, normality and equal variance were tested using the Shapiro–Wilk (Royston 1982) and Brown–Forsythe (Brown and Forsythe 1974) tests, respectively. All analyses were performed using SigmaPlot 14.0.

2.3.2. In situ Dinophysis spp. observations

The significance of differences in the total abundance of *Dinophysis* spp. cells detected *in situ* by the IFCB using side scattering and fluorescence-based triggering methods were tested with a Mann–Whitney U test. A second Mann–Whitney U test was used to test for significant differences in the total abundance of *Dinophysis* cells detected by the IFCB and determined from microscope counts. A permutational multivariate analysis of variance (PERMANOVA, Anderson 2017) was used to test for significant difference in *Dinophysis* species composition determined using the side scattering and fluorescence-based triggering methods. PERMANOVA is a resemblance-based permutational method allowing to perform variance partitioning based on F statistics, like ANOVA, for testing the simultaneous response of several variables to one or several factors with the advantage of not requiring data normality. *Dinophysis* species abundances were fourth root transformed before the PERMANOVA analysis to down-weight the importance of the highly abundant species and to take into account the rarer species in the calculation of the similarity matrix. The PERMANOVA analysis was based on a Bray-Curtis similarity matrix and 9999 permutations were run. The PERMANOVA analysis was performed with the function "adonis" available in the R vegan package (Oksanen et al., 2018). A linear regression model was used to study the relationship between the IFCB-autofluorescence level and biovolume of *Dinophysis* species cells with the function "lm" available in the R stats package. Spearman's correlation was used to evaluate the relationship between the biovolume and IFCB-autofluorescence of *Mesodinium* spp. cells using the function "cor.test" available in the R stats package.

3. Results

3.1. Optimization of IFCB settings

Different PMT gain and threshold setting combinations significantly affected the detection of *D. acuminata* cells in culture by the IFCB using either side scattering or fluorescence-based triggering methods. For both methods, *D. acuminata* abundance estimates were significantly different for the tested setting combinations and there was a significant interaction between the PMT gain and threshold (two-way ANOVA $p < 0.01$ Tables S1 and S2, Fig. 2).

For side scattering image acquisition, PMT A gain settings of 0.30 and 0.40 V underestimated *D. acuminata* abundance for all of the threshold (trig A) settings evaluated (one-way ANOVA, $p < 0.05$ Table S3, Fig. 2A). A PMT A gain setting of 0.30 V only detected 6–26 % of the *D. acuminata* abundance determined microscopically, and a PMT A gain setting of 0.40 V detected 54–80 % of *D. acuminata* abundance. PMT A gain settings of 0.50 and 0.60 V provided *D. acuminata* abundance estimates not significantly different from the microscopic counts for all of the trig A settings evaluated except with the combination of PMT A gain = 0.60 V and trig $A = 0.25$ V which resulted in a higher abundance (Table S3, Fig. 2A). The PMT gain and threshold settings also influenced the effective volume analyzed and total number of particles detected by the IFCB with a significant interaction between the PMT A gain voltage and trig A voltage (two-way ANOVA $p < 0.001$ Tables S4 and S5, Fig. 2C & E). Increasing the PMT A gain voltage resulted in a

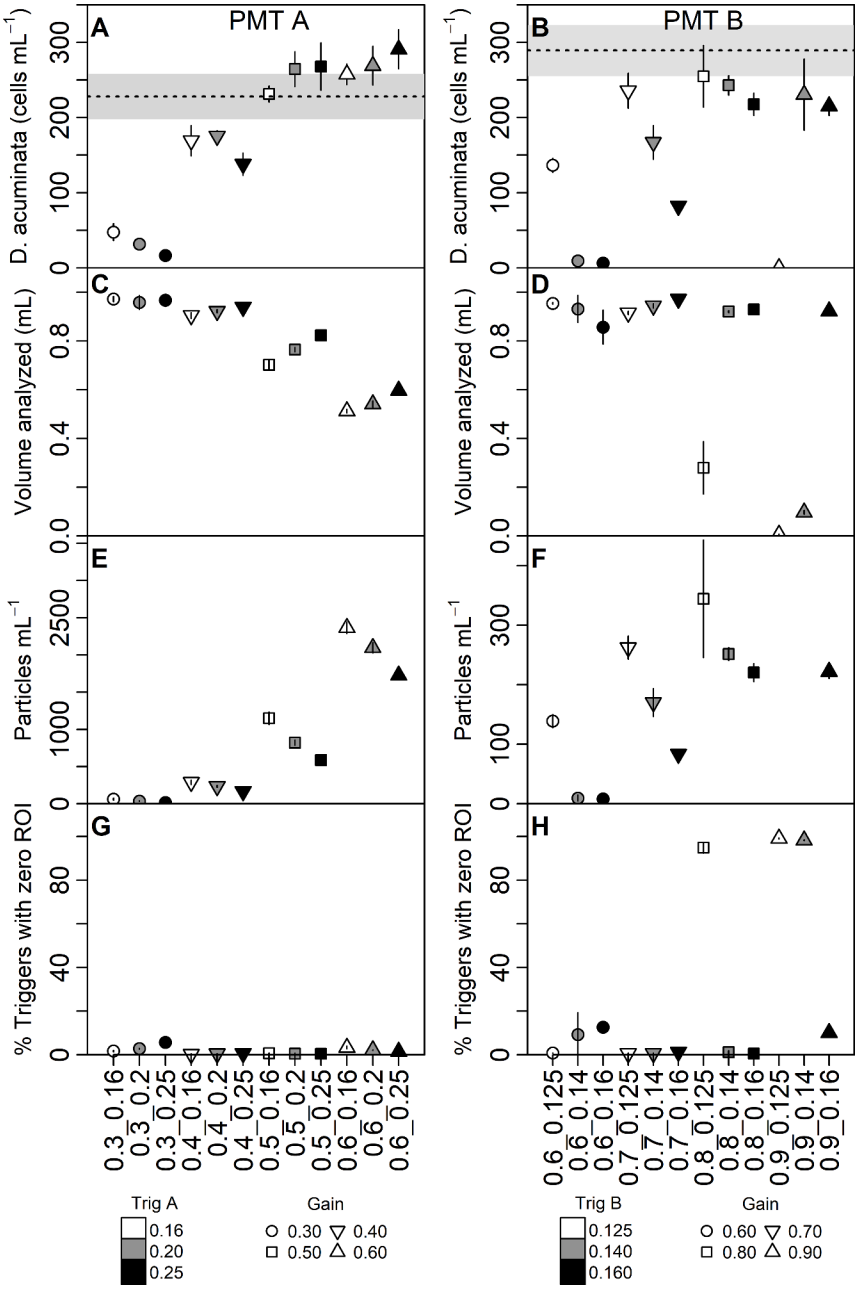

Fig. 2. *Dinophysis acuminata* abundance detected (A & B), effective volume analyzed (C & D) and total number of particles detected (E & F) by the IFCB when triggering the image acquisition on side scattering (left panel) or fluorescence (right panel) using different combinations of photomultiplier tubes (PMTs) gains (symbols) and thresholds (colors) settings. Side scattering gains tested: 0.3, 0.4, 0.5 and 0.6. Side scattering thresholds tested: 0.16, 0.20 and 0.25. Fluorescence gains tested: 0.6, 0.7, 0.8 and 0.9. Fluorescence thresholds tested: 0.125, 0.14 and 0.16. Horizontal dashed line corresponds to the microscopic count and gray highlight represents Willén (1976)'s error rate.

lower effective volume analyzed and higher number of (non-target/uninteresting) particles detected. For a given PMT A gain voltage, the effective volume analyzed was proportional to the trig A voltage, while the total number of particles detected was inversely proportional to the trig A voltage. Some trig A combinations with the PMT A gain = 0.50 and 0.60 V settings were so sensitive to small particles in the *D. acuminata* culture that the effective volume analyzed was only 0.51–0.68 mL instead of the 1 mL that the IFCB was programmed to sample.

For fluorescence-based image acquisition, *D. acuminata* abundance was underestimated in comparison to the microscopic counts for all PMT gain and threshold setting combinations except for the combination of PMT B gain = 0.80 V and threshold trig $B = 0.125$ V (Fig. 2B, one-way ANOVA $p < 0.05$ Table S6). The PMT B gain settings of 0.60 and 0.70 V provided the lowest abundance estimates, only detecting 1–51 % and 26–87 % of *D. acuminata* cells respectively. *D. acuminata* abundance estimates obtained with the PMT B gain settings = 0.80 V and 0.90 V were not significantly different from each other and were closest to the microscopic counts. However, when these gain settings were combined with the lowest thresholds (trig $B = 0.140$ and 0.125 V), sometimes the acquisition of images was triggered but no particle was detected on the images. IFCB users call this phenomenon "triggers with zero region of interest (ROI)". This can occur for high gain combined with low threshold due to electrical noise that can sometimes be sufficient to trigger image acquisition when there is no real particle. It can also occur for certain combinations of other settings within the IFCB configuration (i.e., blobXgrowAmount, blobYgrowAmount, and minimumBlobArea) when high gain is combined with low threshold settings and tiny debris is detected - in this case, the trigger is real but the ROI is too small to be saved based on the configuration settings. The combination of PMT B gain = 0.90 V and trig $B = 0.140$ V saturated the IFCB with triggers with zero ROI (98 % of triggers with zero ROI Fig. 2H) and the effective volume analyzed was only 0.1 mL of the 1 mL sample (Fig. 2D). The same phenomenon occurred with the combination PMT B gain = 0.80 and trig $B = 0.125$ which only analyzed 0.16–0.36 mL of the 1 mL sample and resulted in 95 % of triggers with zero ROI. With the combination of PMT $B = 0.90$ V and trig $B = 0.125$, the number of triggers with zero ROI was so high that the IFCB was unable to manage them and the software IFCBacquire stopped running before the sample could be completely analyzed. In contrast to PMT B, none of the settings tested for PMT A resulted in a high proportion of triggers with zero ROI (Fig. 2G).

Similarly to the PMT A experiment, the PMT B gain and threshold settings influenced the effective volume analyzed and total number of particles detected by the IFCB with a significant interaction between the PMT B gain voltage and trig B voltage (two-way ANOVA $p < 0.001$ Tables S7 and S8, Fig. 2D & F). Increasing the PMT B voltage resulted in a higher number of particles detected and for a given PMT B voltage, the total number of particles detected was inversely proportional to the trig B voltage; however, contrary to the PMT A experiment, the majority of particles detected were *D. acuminata* cells with just a small number of non target/uninteresting particles (Fig. 2F).

Optimal settings were identified as those that provided abundances not significantly different from the microscopic counts, analyzed the near-total sample volume, and minimized the detection of small debris. The combination of PMT $A = 0.50$ V with trig $A = 0.20$ or 0.25 V was identified as the best setting to detect *D. acuminata* in culture using the side scattering. The best settings to detect *D. acuminata* using the fluorescence triggering were determined to be PMT $B = 0.80$ V and trig $B = 0.140$ V.

The optimal gain and threshold settings identified here for *D. acuminata* in culture correspond to the settings that were used to acquire the existing time series of IFCB observations in Budd Inlet for the side scattering triggering method (PMT $A = 0.50$ V and trig $A = 0.25$ V), but not for fluorescence. The gain setting used for fluorescence-based image acquisition in the field was less sensitive than the setting found to be optimal in the laboratory experiments, but the threshold setting was lower (PMT $B = 0.60$ V and trig $B = 0.125$ V in the field vs. PMT $B = 0.80$ V and trig $B = 0.140$ V in the laboratory for *D. acuminata* in culture).

3.2. *In situ Dinophysis spp. observations*

3.2.1. *Dinophysis spp. and Mesodinium spp. bloom dynamics*

Two blooms of *Dinophysis* spp. were observed by microscopy and the IFCB in Budd Inlet from March 31 to September 27, 2022. The first bloom occurred from June to mid-July ("June–July bloom" hereafter) and was primarily composed of *Dinophysis fortii, D. acuminata*, and *Dinophysis norgevica*. The maximum density of *Dinophysis* spp. detected by the IFCB during the June–July bloom was 4682 cells L^{-1} on June 30th. Weekly microscopy sampling detected 8000 cells L^{-1} two weeks later on July 14th, but IFCB data were not available at that time due to instrument maintenance. The June–July *Dinophysis* spp. bloom was preceded by a bloom of *Mesodinium* spp. that started at the end of May and lasted until the end of June (Fig. 3A & B). The second *Dinophysis* spp. bloom occurred at the end of September ("September bloom" hereafter) and was dominated by *D. fortii* (Fig. 3A & B). The maximum density of *Dinophysis* spp. detected by the IFCB was 6657 cells L^{-1} on September 22nd. The September bloom coincided with a second bloom of *Mesodinium* spp. Two other *Dinophysis* species were observed during the deployment. *Dinophysis parva* was detected at low abundances in July, August, and early September. *Dinophysis odiosa* was detected at low abundances on only two occasions: September 19th and 27th. A small number of dividing and fusing *Dinophysis* spp. cells were detected at the beginning of the June–July bloom and at the end of August (data not shown).

3.2.2. *Side scattering versus fluorescence-based detection of Dinophysis spp. in relation to Mesodinium spp. abundance*

The temporal dynamics of *Dinophysis* spp. abundance determined by the IFCB using side scattering and fluorescence-based triggering methods were similar to one another and were similar to patterns determined from the microscopic counts (Fig. 3A & B); however, in comparison to microscopic counts, the IFCB underestimated the total abundance of *Dinophysis* spp. regardless of the method used to trigger image acquisition (Mann–Whitney U test, $p < 0.05$). Even though the field settings for fluorescence-based image acquisition were found to be less sensitive than the optimal settings identified in the laboratory for *D. acuminata* in culture, there were no significant differences in *Dinophysis* species composition determined using the two triggering methods; that is, both methods performed equally in the detection of all five species of *Dinophysis* observed (PERMANOVA, $p > 0.05$, Fig. 3A & B). However, in some samples, the side scattering triggering method detected more *Mesodinium* spp. cells than the fluorescence triggering method. For example, approximately two times more *Mesodinium* spp. cells were detected using side scattering compared to fluorescence triggering method in June (maximum abundance of 5609 *Mesodinium* spp. cells L^{-1} detected with the side scattering vs. 2460 cells L^{-1} detected by triggering on fluorescence) and September (maximum abundance of 10,636 *Mesodinium* spp. cells L^{-1} detected with the side scattering vs. 4422 cells L^{-1} detected by triggering on fluorescence).

Towards the end of the June–July bloom, there was also a 7-day period when there was a significant difference in the total abundance of *Dinophysis* spp. cells detected using the two triggering methods (Mann–Whitney U test, $p < 0.05$). During this period (highlighted in gray on Fig. 3A & B), the side scattering triggering method detected low abundances of *Dinophysis* spp. cells (the presence of which was confirmed by microscopy) while the fluorescence triggering method did not detect any cells. The proportion of fluorescent *Dinophysis* spp. cells observed by microscopy during this period was the lowest observed during the entire deployment and the level of autofluorescence of *Dinophysis* spp. cells measured by the IFCB decreased (Fig. 3C). The size and level of IFCB-autofluorescence of *Dinophysis* spp. cells were

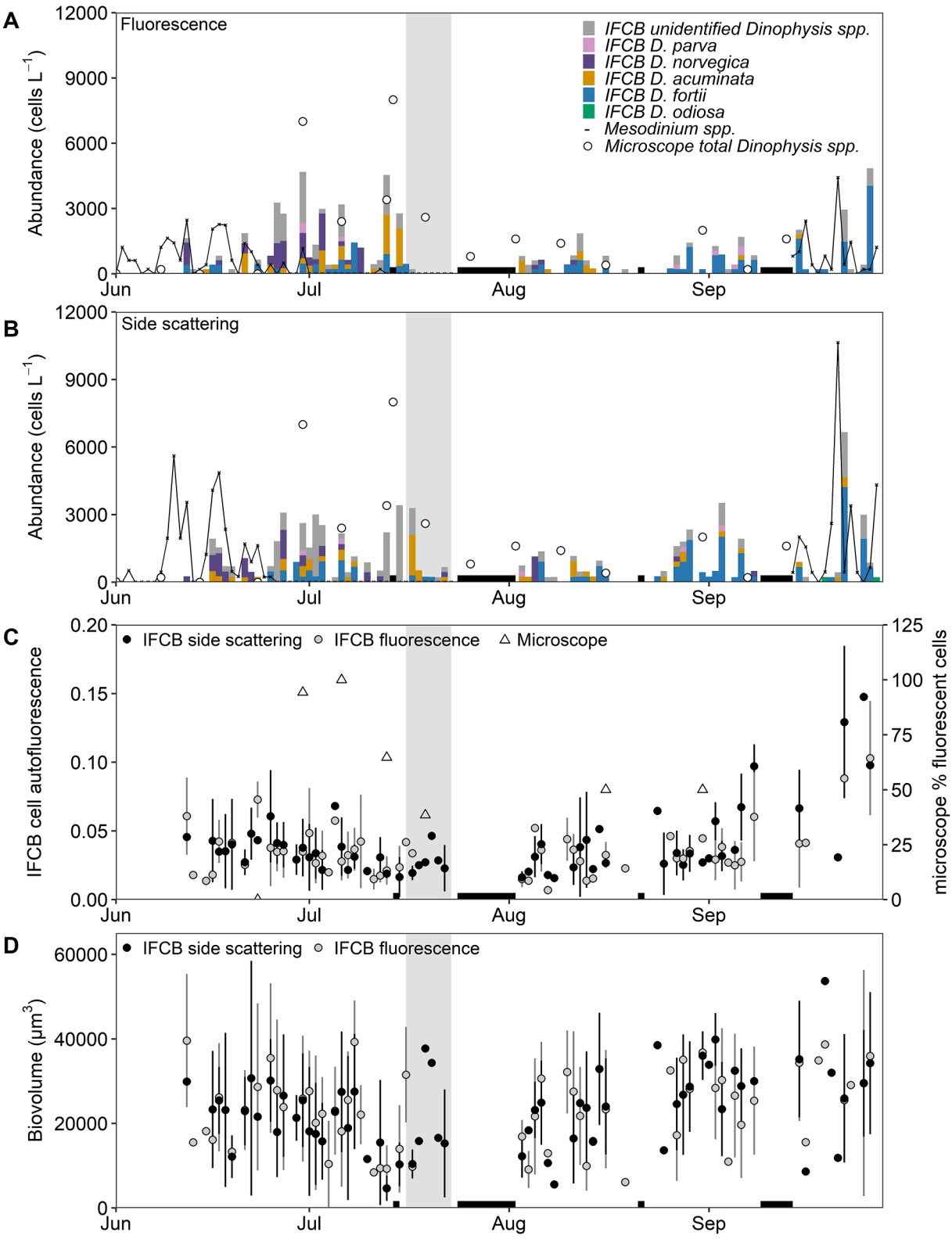

Fig. 3. Temporal dynamics of *Mesodinium* spp. abundance, total *Dinophysis* spp. abundance and *Dinophysis* species composition in Budd Inlet measured with the Imaging FlowCytobot (IFCB) by triggering on fluorescence (A) and side scattering (B). Each time point is one syringe sample. For comparison, total *Dinophysis* spp. abundance obtained by conventional microscopy is also represented. (A) and (B) share the same legend. (C) Temporal variations in the level of autofluorescence of *Dinophysis* spp. cells (mean ± standard deviation) measured by the IFCB (IFCB-autofluorescence) by triggering on fluorescence (white circles) and side scattering (black circles) and percentage of fluorescing *Dinophysis* spp. cells observed by epifluorescence microscopy (white triangles). (D) Biovolume of *Dinophysis* spp. cells (mean ± standard deviation) measured by the IFCB by triggering on fluorescence and side scattering. Black bars on the x-axis indicate IFCB data gaps. The gray shaded area highlights a period when the IFCB detected *Dinophysis* spp. cells when side scattering was used to trigger the image acquisition while triggering on fluorescence did not.

significantly and positively correlated (Fig. 4), but this correlation only explained 28 % of the variability and did not explain the difference in detection of *Dinophysis* spp. cells between the two triggering methods observed during this 7-day period. Indeed, while there were some samples with *Dinophysis* spp. cells presenting a low biovolume (<20,000 μm^3) during this period, there were also samples with cells presenting a high biovolume (31,513–37,718 μm^3). Further, at other times during the deployment, some *D. fortii* with similar size presented very different levels of IFCB-autofluorescence. This suggests that the physiological status of the *Dinophysis* spp. cells may have contributed to variability in their autofluorescence which resulted in the inability of the IFCB to detect them when triggering on fluorescence.

The level of IFCB-autofluorescence of *Dinophysis* spp. cells and proportion of *Dinophysis* spp. cells exhibiting fluorescence observed by microscopy (Fig. 3C) covaried with the abundance of *Mesodinium* spp. (Fig. 3A & B). In June, when *Dinophysis* spp. co-occurred with *Mesodinium* spp., the level of IFCB-autofluorescence of *Dinophysis* spp. cells ranged from 0.007 to 0.094. After the disappearance of *Mesodinium* spp. in July, the level of IFCB-autofluorescence of *Dinophysis* spp. cells progressively decreased and reached a minimum average value of 0.015. IFCB-autofluorescence levels of *Dinophysis* spp. cells remained relatively low until September when they reached the highest levels observed during the deployment, coinciding with the second bloom of *Mesodinium* spp. and the September bloom of *Dinophysis* spp.

A wide range of *Mesodinium* spp. cell sizes were observed during the deployment, with biovolume ranging from 28 to 59,051 μm^3 (Fig. 5A). The first bloom of *Mesodinium* spp. presented a wider range in cell size than the second bloom, but the majority of *Mesodinium* spp. cells measured 28–10,000 μm^3. In contrast, during the second bloom, the majority of *Mesodinium* spp. cells presented a bigger size (5000–15,000 μm^3). The biovolume and level of IFCB-autofluorescence of *Mesodinium* spp. cells were positively correlated ($r = 0.71$, $p < 0.001$) (Fig. 5B).

4. Discussion

The IFCB failed to detect *Dinophysis* spp. *in situ* using the fluorescence triggering method when the IFCB-autofluorescence level of individual cells was low and when the proportion of cells exhibiting autofluorescence determined by microscopy was less than 50 %. This was observed during a 7-day period towards the end of the June–July bloom, when cells were still detected using the side scattering triggering method. It is worth noting that the IFCB gain and threshold settings used in the field were less sensitive than the optimal settings for fluorescence-based image acquisition of *Dinophysis acuminata* determined from the laboratory experiments. In the case of *Dinophysis* spp. and likely other mixotrophic dinoflagellates, PMT B settings for fluorescence-based image acquisition need to be fairly sensitive to detect starved cells and/or the side scattering triggering method may need to be used to ensure their detection. Given the growing interest in using IFCBs to monitor HABs and initiate management actions, robust IFCB calibration procedures, such as the approach used in this study, are critical to ensure accurate detection of HAB species.

The results of this study highlight the importance of intentionally selecting the triggering method (side scattering and/or fluorescence) for image acquisition by the IFCB, as well as quantitatively tuning the gain and threshold settings. Fluorescence-based image acquisition is commonly used for HAB (and phytoplankton) monitoring and detection in nearshore environments to avoid interference by high abundances of detritus; however, this method may not always be suitable for detecting *Dinophysis* spp. and other non-constitutive mixotrophic species like

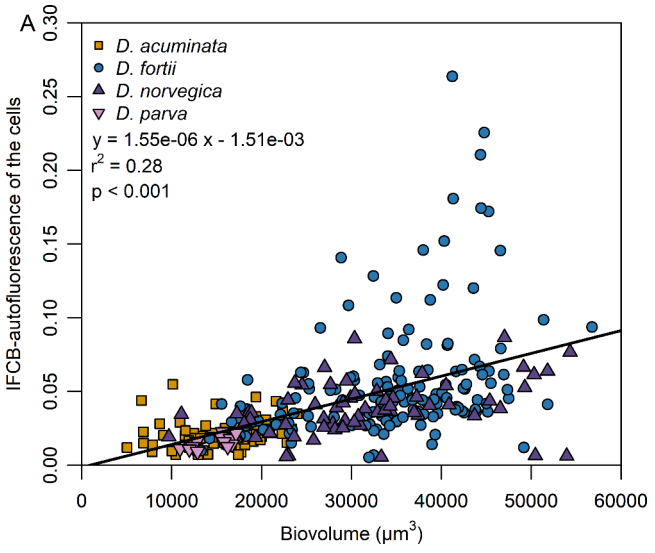

Fig. 4. Level of IFCB-autofluorescence vs. biovolume of *Dinophysis acuminata, Dinophysis fortii, Dinophysis norvegica* and *Dinophysis parva*. Black line represents linear regression.

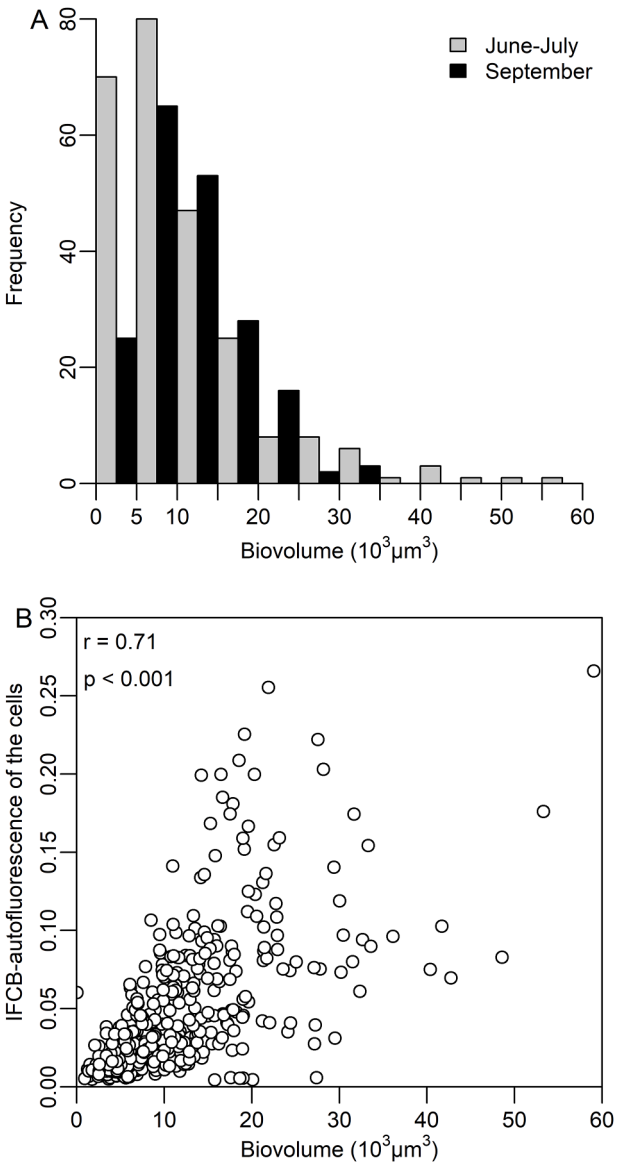

Fig. 5. (A) Histogram of *Mesodinium* spp. biovolume during June–July and September. (B) Level of IFCB-autofluorescence vs. biovolume of *Mesodinium* spp.

Mesodinium spp. or green *Noctiluca scintillans*. The autofluorescence of these species depends on prey availability or physiological status of symbionts. As such, fluorescence-based image acquisition can undercount or entirely miss starved cells exhibiting low or no autofluorescence. In contrast, the side scattering triggering method detects all particles that scatter light and will consequently image non-fluorescing cells that may be missed by the fluorescence-based triggering method. Side scattering may also provide a better understanding of biotic interactions because it will image target HAB species as well as the surrounding community, inclusive of non-fluorescing heterotrophic dinoflagellates and small zooplankton. For example, *in situ* IFCB samples analyzed using the side scattering triggering method in this study detected significantly more *Mesodinium* spp. compared to the fluorescence triggering method, providing insight into predator-prey dynamics. In environments that have high abundances of detritus with a size range close to target HAB species, however, the side scattering triggering method can introduce error due to the inhibit time.

As expected, in this study, inhibit times for *in situ* samples analyzed using the side scattering triggering method were consistently higher than for the fluorescence triggering method with the exception of two samples over the entire deployment duration (data not shown). As a result, the effective volume analyzed by side scattering was on average 0.57 mL less than that analyzed by fluorescence (note that the IFCB was configured to sample 5 mL). These results are representative of an inherent trade-off in selecting a triggering method whereby the fluorescence triggering method typically has lower inhibit times due to reduced interference from detritus but can miss particles with lower autofluorescence. Approaches that IFCB users can consider to balance this trade-off and more accurately detect non-constitutive mixotrophic species like *Dinophysis* spp. during starvation include: 1) alternating triggering between side scattering and fluorescence (as was done in this study), 2) triggering with both side scattering and fluorescence, or 3) increasing the sensitivity of PMT B and pooling samples. Alternating between both triggering methods allow users to take advantage of the lower inhibit times from the fluorescence method, while using the side scattering method to ensure that they are not missing cells exhibiting low or no autofluorescence. For the second option, both PMT channels (PMT A and PMT B) are tuned on and the IFCB triggers with an "OR" logic such that a particle exhibiting low fluorescence (e.g., a starved *Dinophysis* spp. cell) that does not meet the threshold for triggering on PMT B may still trigger on PMT A. In this scenario, careful tuning would be needed to decrease the side scattering sensitivity to filter out small particles and detritus to avoid introducing error due to high inhibit times and to increase the fluorescence sensitivity to more accurately detect prey (i.e., small *Mesodinium* spp.). For the third option, only PMT B would be turned on for sampling but with the fluorescence sensitivity increased to detect weakly fluorescing *Dinophysis* spp. cells. To offset the potential reduced sample volume due to higher inhibit time – a trade-off of increasing sensitivity – multiple samples (i.e., IFCB syringe pulls) could be pooled to get more accurate estimates of species abundances. Of note, a modified version of the IFCB has been developed that carries out automated live cell fluorescent staining to improve the detection of organisms that don't exhibit autofluorescence (IFCB-S; Brownlee et al., 2016). While there are no plans to commercialize the IFCB-S at this time, it represents an important step in the evolution of new strategies for automated detection of starved mixotrophs, like *Dinophysis* spp., or herbivorous microzooplankton.

Once the IFCB triggering method has been chosen, the gain and threshold settings need to be tuned. Two commonly used approaches for tuning the gain and threshold settings of the IFCB are to: 1) image as wide a size range of phytoplankton as possible, or 2) optimize the detection of target species. The best approach will differ depending on the application. For example, tuning the IFCB using the first approach would be most suited if the goal is to study HAB dynamics in relation to the surrounding phytoplankton community. Alternatively, the second tuning approach would be most appropriate if the goal is to accurately quantify a target species and provide early warning of HAB events based on abundance thresholds. Fine tuning the PMT settings using this approach screens out particles that are not of interest and increases the likelihood of detecting target HAB species even when they are present at low abundances. In the case of *Dinophysis* spp., if the goal is to study how the predator/prey relationships influence *Dinophysis* spp. ecology, the PMT settings will need to be adjusted to accurately detect both *Mesodinium* spp. and *Dinophysis* spp.

This study introduces an approach for tuning an IFCB to optimize detection of a target species and demonstrates the effects of a poorly-calibrated IFCB. The most optimal settings were found by iteratively adjusting the PMT gain and threshold settings so that the number of *D. acuminata* cells imaged by the IFCB was as close as possible to the microscope count from the same sample. The laboratory experiments showed that non-optimal settings missed a significant proportion of *D. acuminata* abundance whatever the method used to trigger the images acquisition. *Dinophysis* spp. can present acute toxicity at low abundances (e.g., Yasumoto et al., 1985), so a poorly-calibrated IFCB may not provide HAB early warning. The optimal PMTs gain and threshold settings identified in this study may provide a good starting point for other IFCB users wishing to tune their IFCB to target *Dinophysis* spp. However, due to inherent differences across instruments which make each IFCB a unique instrument, IFCB detection settings are not directly transferable and the users will still need to reproduce the calibration approach presented here with their own instrument. For example, two IFCBs with the same PMT settings deployed in tandem in the Monterey Bay produced different phytoplankton cell concentrations (McGaraghan et al., 2022). Although a single strain culture was used to demonstrate the calibration approach, IFCB settings may also need to be further refined for *in situ* sampling. Natural samples not only have different strains of the target species with variable autofluorescence, but also a diversity of other phytoplankton. For example, when the optimal settings for fluorescence identified in the laboratory study were applied to a discrete, natural sample from Budd Inlet spiked with a known number of cultured *D. acuminata* cells, high abundances of nanoplankton were sampled and the PMT B settings needed to be adjusted down to accurately quantify *D. acuminata* (data not shown). Therefore, while optimal IFCB settings determined using cultures provide an ideal starting place, further tuning with natural samples may still be required.

The field results of this study demonstrated that the physiological status of *Dinophysis* spp. can influence detection by the IFCB. Overall, both IFCB triggering methods provided a similar view of *Dinophysis* spp. temporal dynamics, except during a 7-day period towards the end of the June–July bloom when fluorescence did not trigger *Dinophysis* spp. cells, but side scattering did. The June–July bloom of *Dinophysis* spp. was preceded by a bloom of *Mesodinium* spp., which started to decline from mid-June until *Mesodinium* spp. was no longer detected in July. After this period, the proportion of fluorescing *Dinophysis* spp. cells determined by microscopy and autofluorescence of individual cells measured with the IFCB progressively decreased, and reached their lowest point when the IFCB fluorescence triggering method did not detect any *Dinophysis* spp. cells, but the scattering triggering method did. Together, this suggests that starved *Dinophysis* spp. cells were not adequately detected by the IFCB.

The decrease in autofluorescence of *Dinophysis* spp. cells observed by microscopy and by the IFCB about one month after the decline of the *Mesodinium* spp. bloom is in line with findings from laboratory experiments showing the effect of starvation on *D. fortii* and *D. caudata* (Nagai et al., 2008; Park et al., 2008). These studies showed that in absence of prey, the plastids that *D. fortii* and *D. caudata* previously sequestered remained functional for 1–2 months but the autofluorescence of the cells and their photosynthetic ability decreased during the starvation. Of note, starved *D. caudata* cells can reacquire plastids and recover their autofluorescence as soon as one day after addition of *Mesodinium rubrum* in the laboratory cultures (Park et al., 2008). In a field setting, this rapid recovery of autofluorescence, and hence detection by the IFCB using

fluorescence triggering, could complicate efforts to determine the source of *Dinophysis* spp. cells and understand bloom initiation and predator-prey dynamics (e.g., whether *Dinophysis* spp. cells were advected into a region or a local population of starved cells were exposed to prey).

The highest values of IFCB-autofluorescence of *Dinophysis* spp. cells were observed during the September bloom. In contrast to the June–July bloom of *Dinophysis* spp., which lagged peak abundances of *Mesodinium* spp., the September bloom of *Dinophysis* spp. co-occurred with a bloom of large *Mesodinium* spp. The presence of *Mesodinium* spp. throughout the September bloom would have provided a sustained source of plastids that *Dinophysis* spp. could acquire, thus increasing autofluorescence. Additionally, the biovolume of *Mesodinium* spp. cells were found to be positively correlated with their IFCB-autofluorescence, demonstrating that larger cells of *Mesodinium* spp. have more plastids. The larger and more nutritious cells of *Mesodinium* spp. during the September bloom provide another reason for the high levels of *Dinophysis* spp. IFCB-autofluorescence. This finding is supported by laboratory (Smith et al., 2018) and field studies (Harred and Campbell 2014), which have observed that larger *Mesodinium* spp. cells are more nutritious and support faster growth rates and higher biomass of *Dinophysis* spp. However, the potential for other environmental factors, such as light intensity (Nielsen et al., 2012) and nutrient availability (Parkhill et al., 2001), to influence the autofluorescence of *Dinophysis* spp. cells cannot be ruled out. A controlled laboratory experiment would be needed to explore the effect of starvation on detection of *Dinophysis* spp. cells by the IFCB in the absence of other variables.

To avoid acute health risks, it is essential that IFCB monitoring programs can accurately detect both starved cells with reduced autofluorescence and low cell abundances, because starved cells can still contain toxins. Laboratory experiments have found higher cellular toxin quotas for DSTs (i.e., okadaic acid, dinophysistoxin-1b, dinophysistoxin-2 and pectenotoxin-2) in prey-depleted, senescent cultures compared to well-fed, exponentially growing cultures (García-Portela et al., 2018; Nielsen et al., 2012; Nielsen et al., 2013). This occurs because toxin production continues while growth rates decline, resulting in an accumulation of toxins in cells. Evidence of this has also been found in the field (e.g., Pizarro et al., 2008). It is the product of *Dinophysis* spp. cell abundance and cell toxicity that influences shellfish toxicity and the resulting risk for DSP (García-Altares et al., 2016; Reguera et al., 2014) but high abundances are not a requirement for *Dinophysis* spp. cells representing a risk. For instance, Lindahl et al. (2007) indicated that approximately 100 highly toxic cells from a low-density population of *D. acuminata* may lead to the same accumulation of DST in a mussel as the ingestion of 1500 low toxic cells from a higher density population. Further, because *Dinophysis* spp. can reacquire plastids after a period of starvation (Park et al., 2008), in the field, such populations of highly-toxic prey-limited *Dinophysis* spp. could become a "seed" population able to recover and potentially bloom after the return of *Mesodinium* spp.

5. Conclusion

The IFCB is increasingly being used to rapidly and autonomously detect developing HABs *in situ* and provide insight into aspects of HAB ecology. It is therefore important to consider best practices and develop standardized approaches to ensure accurate detection of HAB species and facilitate comparison of IFCB data products across instruments and user groups. This study demonstrates a quantitative approach to tune the IFCB settings to optimize detection of a target HAB taxon and highlights the trade-offs associated with choosing a triggering method for image acquisition. Fluorescence-based image acquisition in environments with high detritus will lower inhibit times relative to side scattering, but may miss the detection of non-constitutive mixotrophic species like *Dinophysis* spp. when prey is limited. If the target HAB is a mixotrophic species, one path forward is to alternate sampling with the fluorescence and side scattering triggering methods. Having both types of measurements in this study allowed us to determine that the temporary disappearance of *Dinophysis* spp. from the fluorescence triggering record was likely caused by starvation. Given the effect that IFCB settings have on data quality, users should consider reporting both their calibration procedure and IFCB settings to better compare measurements across the IFCB user community.

Funding

This paper is a result of research funded by the National Oceanic and Atmospheric Administration National Centers for Coastal Ocean Science Competitive Research Program under award NA19NOS4780182 to the Virginia Institute of Marine Science. E.H. was awarded a Fulbright Fellowship funded by the Franco-American Fulbright Commission and French region Hauts-de-France. This is ECOHAB publication number ECO1084.

Declaration of Competing Interest

The authors declare that they have no known competing financial interests or personal relationships that could have appeared to influence the work reported in this paper.

Data availability

Data will be made available on request.

Acknowledgements

We thank Nour Ayache, Megan Ladds, James Fiorendino and Lisa Campbell for providing isolates of *Dinophysis* spp., *Mesodinium rubrum,* and *Teleaulax amphioxeia* and for their precious advice on *Dinophysis* spp. culturing. For their technical assistance with IFCB maintenance, we thank Tom Fougere, Vinnie Ferreira and Ivory Engstrom. We thank Mark Fleischer for providing access to his boathouse and Vera Trainer for support during the IFCB field deployment and assistance in the writing of the Fulbright proposal.

Supplementary materials

Supplementary material associated with this article can be found, in the online version, at doi:10.1016/j.hal.2023.102544.

References

Anderson, D.M., Andersen, P., Bricelj, V.M., Cullen, J.J., Rensel, J.E.J., 2001. Monitoring and management strategies for harmful algal blooms in coastal waters, APEC #201-MR-01.1, Asia Pacific Economic Program, Singapore, and Intergovernmental Oceanographic Commission Technical Series No. 59, Paris.

Anderson, D.M., Cembella, A.D., Hallegraeff, G.M., 2012. Progress in understanding harmful algal blooms: paradigm shifts and new technologies for research, monitoring, and management. Annu. Rev. Mar. Sci. 4 (1), 143–176.

Anderson, D.M., Fensin, E., Gobler, C.J., Hoeglund, A.E., Hubbard, K.A., Kulis, D.M., Landsberg, J.H., Lefebvre, K.A., Provoost, P., Richlen, M.L., Smith, J.L., Solow, A.R., Trainer, V.L., 2021. Marine harmful algal blooms (HABs) in the United States: history, current status and future trends. Harmful Algae 102, 101975.

Anderson, M.J., 2017. Permutational Multivariate Analysis of Variance (PERMANOVA). Wiley StatsRef, pp. 1–15. Statistics Reference Online.

Ayache, N., Bill, B.D., Brosnahan, M.L., Campbell, L., Deeds, J.R., Fiorendino, J.M., Gobler, C.J., Handy, S.M., Harrington, N., Kulis, D.M., McCarron, P., Miles, C.O., Moore, S.K., Nagai, S., Trainer, V.L., Wolny, J.L., Young, C.S., Smith, J.L., 2023. A survey of *Dinophysis* spp. and their potential to cause diarrhetic shellfish poisoning in coastal waters of the United States. J. Phycol. 00, 1–23.

Belin, C., Soudant, D., Amzil, Z., 2021. Three decades of data on phytoplankton and phycotoxins on the French coast: lessons from REPHY and REPHYTOX. Harmful Algae 102, 101733.

Boatman, C., Cox, J.M., Devol, A., Ebbesmeyer, C.C., Edinger, J., Newton, J., Norton, D., 2000. Budd Inlet Scientific Study: An Overview of Findings. LOTT Wastewater Resource Management Plan, p. 8.

Brown, C.W., Green, D., Hickey, B.M., Jacobs, J.M., Lanerolle, L.W.J., Moore, S.K., Schwab, D.J., Trainer, V.L., Trtanj, J., Turner, E.J., Wood, R., Wynne, T., 2012. Towards operational forecasts of algal blooms and pathogens. In: Morain, S.A., Budge, A.M. (Eds.), Environmental Tracking for Public Health Surveillance. CRC Press, pp. 345–368.

Brown, M.B., Forsythe, A.B., 1974. Robust tests for the equality of variances. J. Am. Stat. 69 (346), 364–367.

Brownlee, E.F., Olson, R.J., Sosik, H.M., 2016. Microzooplankton community structure investigated with imaging flow cytometry and automated live-cell staining. Mar. Ecol. Prog. 550, 65–81.

Campbell, L., Olson, R.J., Sosik, H.M., Abraham, A., Henrichs, D.W., Hyatt, C.J., Buskey, E.J., 2010. First harmful *Dinophysis* (Dinophyceae, Dinophysiales) bloom in the U.S. is revealed by automated imaging flow cytometry. J. Phycol. 46 (1), 66–75.

FDA, 2011. Fish and fishery products hazards and controls guidance. Appendix 5 FDA and EPA Safety Levels in Regulations and Guidance.

García-Altares, M., Casanova, A., Fernández-Tejedor, M., Diogène, J., de la Iglesia, P., 2016. Bloom of *Dinophysis* spp. dominated by *D. sacculus* and its related diarrhetic shellfish poisoning (DSP) outbreak in Alfacs Bay (Catalonia, NW Mediterranean Sea): identification of DSP toxins in phytoplankton, shellfish and passive samplers. Reg. Stud. 6, 19–28.

García-Portela, M., Reguera, B., Sibat, M., Altenburger, A., Rodríguez, F., Hess, P., 2018. Metabolomic profiles of *Dinophysis acuminata* and *Dinophysis acuta* using non-targeted high-resolution mass spectrometry: effect of nutritional status and prey. Mar. Drugs 16 (5), 143.

Glibert, P.M., Pitcher, G.C., Bernard, S., Li, M., 2018. Advancements and continuing challenges of emerging technologies and tools for detecting harmful algal blooms, their antecedent conditions and toxins, and applications in predictive models. In: Glibert, P.M., Berdalet, E., Burford, M.A., Pitcher, G.C., Zhou, M. (Eds.), Global Ecology and Oceanography of Harmful Algal Blooms. Springer International Publishing, Cham, pp. 339–357.

Hansen, P.J., Nielsen, L.T., Johnson, M., Berge, T., Flynn, K.J., 2013. Acquired phototrophy in *Mesodinium* and *Dinophysis* – a review of cellular organization, prey selectivity, nutrient uptake and bioenergetics. Harmful Algae 28, 126–139.

Harred, L.B., Campbell, L., 2014. Predicting harmful algal blooms: a case study with *Dinophysis ovum* in the Gulf of Mexico. J. Plankton Res. 36 (6), 1434–1445.

Hattenrath-Lehmann, T.K., Marcoval, M.A., Berry, D.L., Fire, S., Wang, Z., Morton, S.L., Gobler, C.J., 2013. The emergence of *Dinophysis acuminata* blooms and DSP toxins in shellfish in New York waters. Harmful Algae 26, 33–44.

Holm, S., 1979. A simple sequentially rejective multiple test procedure. Scand. J. Stat. 6 (2), 65–70.

Jin, D., Hoagland, P., 2008. The value of harmful algal bloom predictions to the nearshore commercial shellfish fishery in the Gulf of Maine. Harmful Algae 7 (6), 772–781.

Kim, M., Nam, S.W., Shin, W., Coats, D.W., Park, M.G., 2012. *Dinophysis caudata* (Dinophyceae) sequesters and retains plastids from the mixotrophic ciliate prey *Mesodinium rubrum*. J. Phycol. 48 (3), 569–579.

Kudela, R.M., Anderson, C., Ruhl, H., 2021. The California harmful algal bloom monitoring and alert program: a success story for coordinated ocean observing. Oceanography 34 (4), 84–85.

Lindahl, O., Lundve, B., Johansen, M., 2007. Toxicity of *Dinophysis* spp. in relation to population density and environmental conditions on the Swedish west coast. Harmful Algae 6 (2), 218–231.

Lloyd, J.K., Duchin, J.S., Borchert, J., Quintana, H.F., Robertson, A., 2013. Diarrhetic shellfish poisoning, Washington, USA, 2011 Emerg. Infect. Dis. 19 (8), 1314.

McGaraghan, A., Hayashi, K., Daniel, P., Kudela, R.M., 2022. Development and comparison of Imaging FlowCytobot classifiers in coastal California. In: Band-Schmidt, C.J., Rodríguez-Gómez, C.F. (Eds.), Proceedings of the 19th International Conference on Harmful Algae. La Paz, B.C.S., Mexico. International Society for the Study of Harmful Algal Blooms, pp. 220–224.

Moberg, E.A., Sosik, H.M., 2012. Distance maps to estimate cell volume from two-dimensional plankton images. Limnol. Oceanogr.: Methods 10 (4), 278–288.

Nagai, S., Nitshitani, G., Tomaru, Y., Sakiyama, S., Kamiyama, T., 2008. Predation by the toxic dinoflagellate *Dinophysis fortii* on the ciliate *Myrionecta rubra* and observation of sequestration of ciliate chloroplasts. J. Phycol. 44 (4), 909–922.

NCCOS and US IOOS, 2020. Framework for the national harmful algal bloom observing network: a workshop report. National Centers for Coastal Ocean Science, p. 59.

Neeley, A., Beaulieu, S., Proctor, C., Cetinić, I., Futrelle, J., Soto Ramos, I., Sosik, H., Devred, E., Karp-Boss, L., Picheral, M., 2021. Standards and practices for reporting plankton and other particle observations from images. 38pp.

Nielsen, L.T., Krock, B., Hansen, P.J., 2012. Effects of light and food availability on toxin production, growth and photosynthesis in *Dinophysis acuminata*. Mar. Ecol. Prog. 471, 37–50.

Nielsen, L.T., Krock, B., Hansen, P.J., 2013. Production and excretion of okadaic acid, pectenotoxin-2 and a novel dinophysistoxin from the DSP-causing marine dinoflagellate *Dinophysis acuta* – effects of light, food availability and growth phase. Harmful Algae 23, 34–45.

Oksanen, J., Blanchet, G., Friendly, M., Roeland, K., Legendre, P., McGlinn, D., Minchin, P., O'Hara, R., Simpson, G., Solymos, P., Stevens, H., Szoecs, E., Wagner, H., 2018. vegan: community ecology package. R package version 2.5-3. https://CRAN.R-project.org/package=vegan.

Olson, R.J., Sosik, H.M., 2007. A submersible imaging-in-flow instrument to analyze nano-and microplankton: imaging FlowCytobot. Limnol. Oceanogr.: Methods. 5 (6), 195–203.

Park, M.G., Kim, S., Kim, H.S., Myung, G., Kang, Y.G., Yih, W., 2006. First successful culture of the marine dinoflagellate *Dinophysis acuminata*. Aquat. Microb. Ecol. 45 (2), 101–106.

Park, M.G., Park, J.S., Kim, M., Yih, W., 2008. Plastid dynamics during survival of *Dinophysis caudata* without its ciliate prey. J. Phycol. 44 (5), 1154–1163.

Parkhill, J.-P., Maillet, G., Cullen, J.J., 2001. Fluorescence-based maximal quantum yield for PSII as a diagnostic of nutrient stress. J. Phycol. 37 (4), 517–529.

Pizarro, G., Escalera, L., González-Gil, S., Franco, J.M., Reguera, B., 2008. Growth, behaviour and cell toxin quota of *Dinophysis acuta* during a daily cycle. Mar. Ecol. Prog. 353, 89–105.

PSEMP Marine Waters Workgroup, 2017. In: Moore, S.K., R.W., K.Stark, Bos, J., Williams, P., Hamel, N., Edwards, A., et al. (Eds.), Puget Sound Marine Waters: 2016 Overview.

Reguera, B., Riobó, P., Rodríguez, F., Díaz, P.A., Pizarro, G., Paz, B., Franco, J.M., Blanco, J., 2014. *Dinophysis* toxins: causative organisms, distribution and fate in shellfish. Mar. Drugs 12 (1), 394–461.

Reguera, B., Velo-Suárez, L., Raine, R., Park, M.G., 2012. Harmful *Dinophysis* species: a review. Harmful Algae 14, 87–106.

Royston, J.P., 1982. An extension of Shapiro and Wilk's W test for normality to large samples. J. R. Stat. Soc. 31 (2), 115–124.

Smith, J.L., Tong, M., Kulis, D., Anderson, D.M., 2018. Effect of ciliate strain, size, and nutritional content on the growth and toxicity of mixotrophic *Dinophysis acuminata*. Harmful Algae 78, 95–105.

Sosik, H.M., Olson, R.J., 2007. Automated taxonomic classification of phytoplankton sampled with imaging-in-flow cytometry. Limnol. Oceanogr.: Methods 5 (6), 204–216.

Trainer, V.L., King, T.L., 2023. SoundToxins: a research and monitoring partnership for harmful phytoplankton in Washington State. Toxins (Basel) 15 (3), 189.

Trainer, V.L., Moore, L., Bill, B.D., Adams, N.G., Harrington, N., Borchert, J., da Silva, D. A.M., Eberhart, B.-T.L., 2013. Diarrhetic shellfish toxins and other lipophilic toxins of human health concern in Washington State. Mar. Drugs 11 (6), 1815–1835.

Trainer, V.L., Suddleson, M., 2005. Monitoring approaches for early warning of domoic acid events in Washington State. Oceanography 18 (2), 228–237.

Washington Sea Grant, 2015. Shellfish aquaculture in Washington State. Final report to the Washington State legislature 84p.

Willén, E., 1976. A simplified method of phytoplankton counting. Br. Phycol. J. 11 (3), 265–278.

Yasumoto, T., Murata, M., Oshima, Y., Sano, M., Matsumoto, G.K., Clardy, J., 1985. Diarrhetic shellfish toxins. Tetrahedron 41 (6), 1019–1025.